Journal of Glaciology

Article

Cite this article: Das S, Ramsankaran R (2025) In-situ bathymetry and volume estimation of four glacial lakes in western Himalaya. *Journal of Glaciology* **71**, e95, 1–18. https://doi.org/10.1017/jog.2025.10082

Received: 14 April 2025
Revised: 12 August 2025
Accepted: 15 August 2025

Keywords:
bathymetry; glacial lakes; GLOF hazard assessment; lake volume; uncrewed surface vehicle

Corresponding author: Suresh Das;
Email: sureshdas088@gmail.com;
RAAJ Ramsankaran;
Email: ramsankaran@civil.iitb.ac.in

In-situ bathymetry and volume estimation of four glacial lakes in western Himalaya

Suresh Das and RAAJ Ramsankaran

Hydro-Remote Sensing Applications (H-RSA) Group, Department of Civil Engineering, Indian Institute of Technology Bombay, Powai, India

Abstract

Glacial lakes in the Himalayas have expanded significantly in recent decades, increasing the potential risk of outburst floods. However, limited field surveys and systematic assessments leave downstream communities vulnerable. Accurate volume estimation of glacial lakes is essential for modelling flood dynamics, yet in-situ bathymetric data remain scarce. In this study, we surveyed four glacial lakes—Kya Tso Lake, Panchi Nala Lake, Gepang Gath Lake and Samudra Tapu Lake—in the Chandrabhaga basin, western Himalayas. Depth measurements were conducted using a portable inflatable kayak in August 2022 and an echo sounder mounted on an uncrewed surface vehicle in August 2024. Bathymetric modelling revealed maximum depths of 16 m, 10 m, 46 m, and 59 m, with corresponding storage capacities of 0.89, 0.44, 24.12, and 24.69 × 10^6 m^3, respectively. Volume estimates derived from empirical equations showed substantial discrepancies of ± 36–1736% compared to in-situ measurements. Despite several operational challenges, this study provides valuable in-situ bathymetric data for future modelling and hazard assessment of rapidly expanding glacial lakes in the region. The findings emphasise the need for robust field-based bathymetric datasets to refine empirical volume estimation models for Himalayan glacial lakes.

1. Introduction

Glacial lakes serve as an indicator of climate change (Moser and others, 2019). The formation of glacial lakes can initiate positive feedback mechanisms (Tweed and Carrivick, 2015), where the presence of lakes accelerates ice loss through processes such as calving and subaqueous melting (Carrivick and Tweed, 2013; Sutherland and others, 2020). This, in turn, leads to increased melting and glacier retreat (King and others, 2019; Watson and others, 2020), further contributing to lake expansion (Carrivick and others, 2020). In the Himalayas, numerous glacial lakes, especially moraine-dammed ones, have recently formed and expanded around alpine glaciers (Zhang and others, 2015, 2023a; Shugar and others, 2020). These growing lakes are often bordered by steep slopes and held by fragile moraines, which are susceptible to failure (Westoby and others, 2014). Catastrophic events such as rockfalls, glacier calving, and avalanches into the lake can generate large waves and trigger flooding due to outbursts (Byers and others, 2019; Fischer and others, 2021).

Over the past decades, numerous large Glacial Lake Outburst Floods (GLOFs) have occurred in the Himalayan region (Nie and others, 2018; Shrestha and others, 2023), which have caused significant damage to downstream communities across the globe (Richardson and Reynolds, 2000; Zhang and others, 2023a; Sattar and others, 2025). Additionally, small-scale GLOFs occur frequently but remain unnoticed due to limited damage or remote locations (ICIMOD, 2011). GLOFs and related events threaten millions of people worldwide (Veh and others, 2019; Taylor and others, 2023), and the frequency of such events is expected to increase in the future (Zheng and others, 2021). The continued ice loss due to climate warming (Kraaijenbrink and others, 2017) and expansion of glacial lakes due to climate change therefore represent a globally important natural hazard that requires urgent attention if future loss of life from GLOFs is to be minimised. Therefore, improved monitoring of glacial lakes and a better understanding of GLOF mechanisms are essential.

Lake volume is an important parameter in GLOF hazard assessments (Fujita and others, 2013; Cook and Quincey, 2015). Precisely estimating the storage capacity of glacial lakes is vital for forecasting flood peak discharge, modelling flood progression, and creating early warning systems. Glacial lakes are most often located in remote places, making it difficult to carry out detailed bathymetric surveys. Consequently, lake depths and volumes for unmeasured lakes are often estimated using Volume–Area (VA) empirical relationships developed mainly from small bathymetric datasets (Huggel and others, 2002; Wang and others, 2012; Loriaux and Casassa, 2013; Muñoz and others, 2020; Zhang and others, 2023b). In the Himalayan region, the harsh climate and remoteness of moraine-dammed lakes often result in a shortage of ground-based monitoring data, particularly regarding lake water depth. To date, in-situ measurements of lake

water depth in the Himalayas have been conducted at only a few glacial lakes, mainly concentrated in the central and eastern Himalayas (Table S1). Most in-situ bathymetry-based studies are concentrated in the Everest region of the Nepal Himalaya (Table S1), with only a few lakes monitored in the Lunana region of the Bhutan Himalaya, and in Tibet (Zhang and others, 2023c).

To the best of our knowledge, only a few lakes in the Indian Himalayas have been surveyed using in-situ bathymetry, including South Lhonak (Sharma and others, 2018), Drang Drung (Ramsankaran and others, 2023) and Neelkanth Lake (Deswal and others, 2020). However, many of these studies relied on manual depth measurements using a rope and canoe, resulting in scattered and spatially limited depth points rather than full-coverage bathymetric surveys. This approach introduces significant uncertainties in volume estimation and lake basin characterisation, affecting hazard assessments. The lack of systematic, high-resolution depth data highlights the need for better in-situ survey strategies. To address these limitations, various approaches have been employed across the Himalayas, including portable echo sounders mounted on kayaks (Ramsankaran and others, 2023), and echo sounders integrated with Uncrewed Surface Vehicle (USV) (e.g. Haritashya and others, 2018; Li and others, 2021; Qi and others, 2022; Duan and others, 2023; Zhang and others, 2023c). Among these, the USV-based survey of glacial lakes is more convenient, efficient and time-effective and provides robust datasets, compared to the conventional manual depth measurements. In this study, we address these gaps by employing a hybrid approach using both USV- and kayak-mounted echo sounders, which enables denser, spatially continuous depth measurements, improving the accuracy and reliability of glacial lake volume estimations in the region.

In recent decades, the western Himalayan region has experienced significant growth of glacial lakes (Allen and others, 2016; Prakash and Nagarajan, 2017; Das and others, 2023, 2024), and several lakes have been categorised as potentially dangerous glacial lakes for future GLOF (Das and others, 2024). The small number of published lake-bathymetry measurements in the western Himalayas has resulted in a limited understanding of the morphology and storage capacity of glacial lakes in this region. In this study, we report the results of the first in-situ surveys conducted on four glacial lakes—Kya Tso Lake (KTL), Panchi Nala Lake (PNL), Gepang Gath Lake (GGL) and Samudra Tapu Lake (STL)—located in the Chandrabhaga basin, western Himalayas, India. First, we used bathymetric data collected with high-resolution (i.e. precision and density of depth measurements) echo sounders mounted on a USV and a kayak to model lake basin morphology using Triangulated Irregular Networks (TIN) and calculate their volumes. We then compared our in-situ volume estimates with those derived from empirical VA relationships, highlighting the observed discrepancies. Lastly, we identified key challenges encountered during USV surveys in high-altitude glacial lakes and provided recommendations for improving future surveys.

2. Study areas

This study investigates four glacial lakes (i.e. KTL, PNL, GGL and STL) in the western Himalayas (Table 1; Fig. 1), selected for their contrasting topographical and morphological settings. All four lakes are fed by temperate glaciers within the greater Himalayan range (Table 1; Fig. 1) and exhibit distinct geomorphic characteristics (Das and others, 2024). KTL is a bedrock-dammed lake that is no longer connected to its parent glacier, while PNL, GGL and STL are moraine-dammed lakes that remain in contact with active glacier termini. These lakes were selected for bathymetric surveys based on accessibility and their alignment with established research frameworks for analysing glacial dynamics. Specifically, GGL and STL were prioritised because they have been classified as potentially dangerous glacial lakes for future lake outburst floods in earlier studies (Allen and others, 2016; Prakash and Nagarajan, 2017; Das and others, 2024), and thus warranted immediate attention for detailed bathymetric assessment. In addition, we included PNL, which is also categorised as moderately susceptible to future outburst floods (Das and others, 2024). KTL, although not classified as currently dangerous, was included to increase the diversity of surveyed lake types—particularly a bedrock-dammed, ice-disconnected lake—thus allowing comparative analysis of contrasting morphological settings. Increasing the number and diversity of lakes with in-situ bathymetric data also supports the development of improved empirical VA relationships and contributes to a more nuanced understanding of lake evolution and outburst flood potential in different geomorphic settings. The characteristics of each lake are discussed below.

2.1. Kya Tso Lake

The KTL, situated at the headwaters of the Tsarap Chhu River (a tributary of the Zanskar River), lies at an elevation of 5144 meters above sea level (m asl; Table 1). The lake spans 445 m east-west and 330 m north-south, forming a bedrock-dammed cirque lake following glacial recession (Fig. 2). As of 2024, KTL is detached from its parent glacier, and the distance between the lake and the parent glacier is ~446 m. Glacier meltwater serves as the lake's primary recharge source. The right flank of the lake features steep slopes with unconsolidated loose sediments, whereas the left flank comprises gently sloping terrain dominated by exposed bedrock (Fig. 2).

From 1971 to 1993, KTL exhibited significant expansion: its length increased from 282 m to 448 m, and its surface area grew from 0.04 km^2 to 0.09 km^2 (Text S1; Tables S3–S5; Fig. S1). However, post-1993, both parameters have stagnated (Tables S3–S5; Fig. S5). This stagnation contrasts with the growth patterns observed in other proglacial lakes across the western Himalayas. While KTL's small size, lack of recent growth, and remote location (far from human settlements/infrastructure) reduce its immediate relevance for hazard assessment, bathymetric data could enhance future VA relationship models, contributing to broader regional datasets.

2.2. Panchi Nala Lake

The PNL is located at the headwaters of the Panchi Nala (nala = stream), a tributary of the Bhaga River in the Chandrabhaga basin (Table 1). It is situated at an altitude of 4560 m asl in 2024, with a length of 420 m from east to west and a width of 285 m from north to south. The lake is dammed by an end moraine. The recharge of PNL occurs mainly from the connected glacier's meltwater. The terminus of Panchi Nala Glacier, with abundant ice cliffs covered by thick debris, stretches into the lake (Fig. 3a). PNL is turbid in nature and characterised by several sediment mounds (Fig. 3b). The lake cuts through the end moraine, having a width of ~3 m as of June 2024 (Fig. 3c).

PNL has evolved significantly in size and length during the last 53 years (Tables S3–S5; Fig. S2). Between 1971 and 2024, the lake's length increased from 101 to 376 m (Text S1; Tables S3–S5; Fig.

Table 1. Characteristics of the studied lakes

Lake name	Kya Tso	Panchi Nala	Gepang Ghat	Samadra Tapu
Lat (°N)	32.72243	32.72315	32.52494	32.49876
Long (°E)	77.41352	77.32943	77.22164	77.54825
Elevation (m asl)	5144	4554	4111	4173
Glacier ID (GLIMS)[a]	G077400E32711N	G086958E27924N	G087008E27832N	G084537E28518N
Area (km^2)[b]	0.1	0.11	1.07	1.63
Length (km)[b]	0.43	0.38	2.49	2.45
Maximum depth (m)	15.75	10.48	46.34	58.62
Average depth (m)	8.97	4.15	22.41	15.34
Volume (10^6 m^3)	0.89	0.45	24.02	24.69
Ice contact	No	Yes	Yes	Yes
Contributing river basins	Zanskar River	Chandrabhaga (Chenab) River	Chandrabhaga (Chenab) River	Chandrabhaga (Chenab) River
Type	Bedrock-dammed lake, no-ice contact, clean water	Moraine-dammed Lake, ice contact, circular shape, with turbid water	Moraine-dammed Lake, ice contact, elongated shape, with clean water	Moraine-dammed Lake, in contact with ice, circular shape, with turbidity

[a]Glacier IDs are obtained from the Global Land Ice Measurements from Space (GLIMS; https://www.glims.org/) inventory.
[b]Area and length were measured for August 2024 (see supplementary information for details).

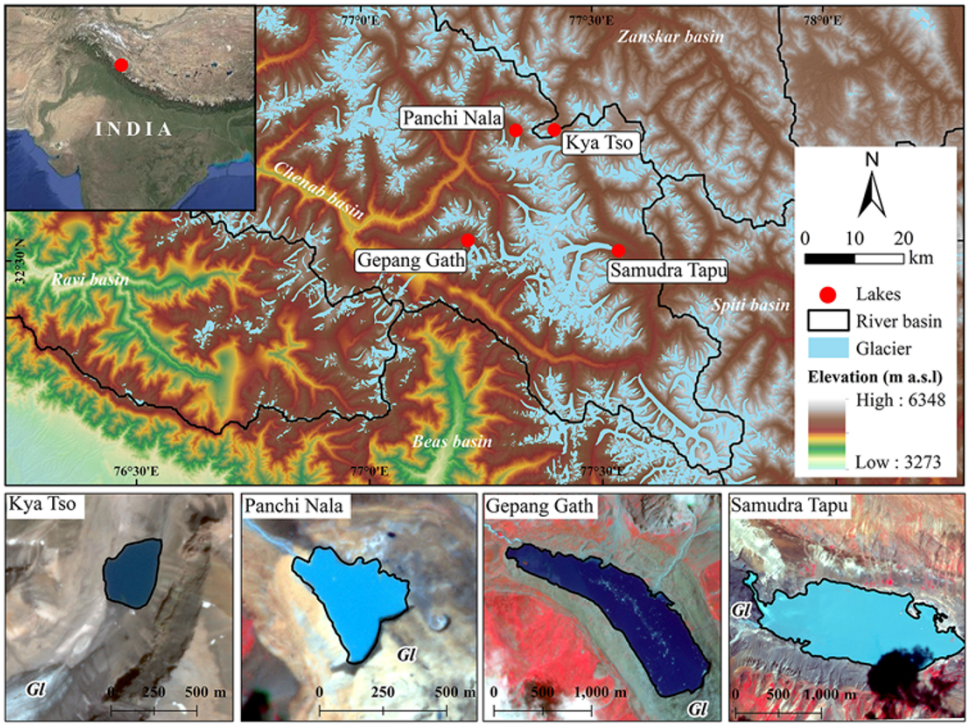

Figure 1. Location of studied glacial lakes in upper Chenab (Panchi Nala, Gepang Gath and Samudra Tapu) and Zanskar (Kya Tso) basins, western Himalaya (upper panel). PlanetScope false colour composite images of glacial lakes as of August 2024 (lower panel). *Gl* = Glacier.

S5), corresponding to an average annual growth rate of 5.18 m a^{-1}, while its area expanded from 0.01 to 0.11 km^2, with an average growth rate of 0.002 km^2 a^{-1} (Tables S3–S5; Fig. S5). Previous studies (Prakash and Nagarajan, 2017; Das and others, 2024) have categorised PNL as moderately susceptible for future lake outburst floods due to several factors, such as the potential for mass movements into the lake from the surrounding steep valley walls and the downstream presence of a meteorological station. A meteorological station, situated ~8 km downstream (~3800 m asl) from the PNL along the Leh–Manali highway, is maintained by the Defence Geoinformatics Research Establishment (Government of India), and houses resident scientists as well as an adjacent Indo-Tibetan Border Police transit camp—underscoring its significance as critical infrastructure potentially exposed to GLOF hazards.

2.3. Gepang Gath Lake

The GGL is one of the top five prioritised glacial lakes in the western Himalayas (Allen and others, 2016; Das and others, 2024). It is situated at an elevation of 4070 m asl, with a length of 2.49 km and a maximum width of 567 m as of 2024 (Table 1). GGL is fed by a ~12.55 km^2 compound valley glacier, which originates from four cirques on the northern slopes of Mount Gepang Goh (~5870 m asl). GGL is bounded by the calving front of the Gepang Gath Glacier to the east, lateral moraines to the north and south and a recessional end moraine to the west (Fig. 4a and b). Ice calving is an active process at GGL (Fig. 4b and c). The lateral moraine trough acts as a 'gutter', trapping debris from rockfalls, snow avalanches and fluvial transport. However, large and rapid mass movements

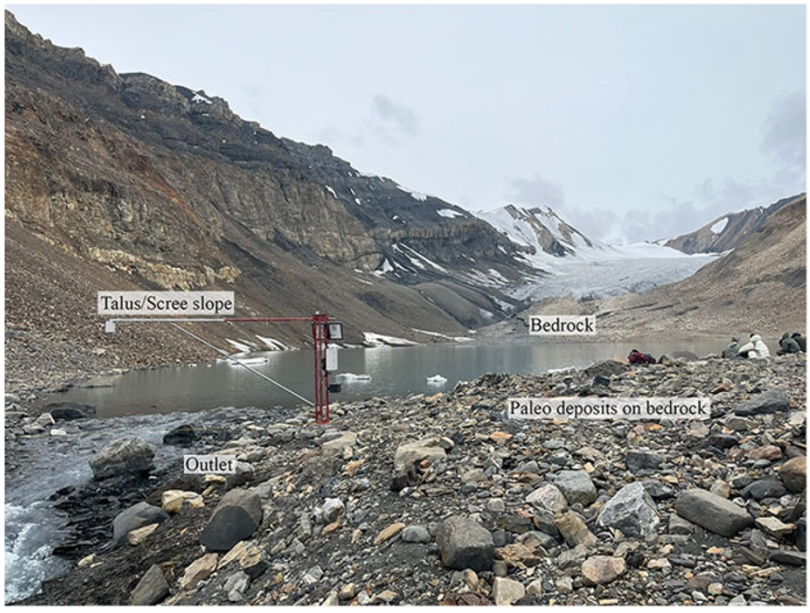

Figure 2. Field photographs of Kya Tso Lake (KTL). KTL is detached from the parent glacier. The outlet is characterised by narrow and shallow channels, mostly occupied by unsorted boulders. The right-side mountain slope of the lake is steeper than the left side, characterised by talus/scree deposits. KTL is a bedrock-dammed cirque lake, formed on palaeo-cirque depressions. A water discharge measurement instrument was installed in August 2024 by the National Centre for Polar and Ocean Research (NCPOR), Govt. of India.

Figure 3. Field photographs of Panchi Nala Lake (PNL). PNL is a pro-glacial lake formed due to the blocking of water by frontal moraine and associated glacial recession. (a) The terminus of PNL as of June 2024 was characterised by exposed ice cliffs. The lake is characterised by several sediment deposits (boulders, sediment mounds), which depict the shallow depth of the lake. (b) View looking towards the up valley. (c) View looking down the valley.

could potentially breach the lateral moraines and enter GGL, posing a significant hazard. The lake outlet is ~6 m wide, and a bridge has been constructed to regulate the outflow, having a freeboard of 5 m as of August 2024 (Fig. 4d and e).

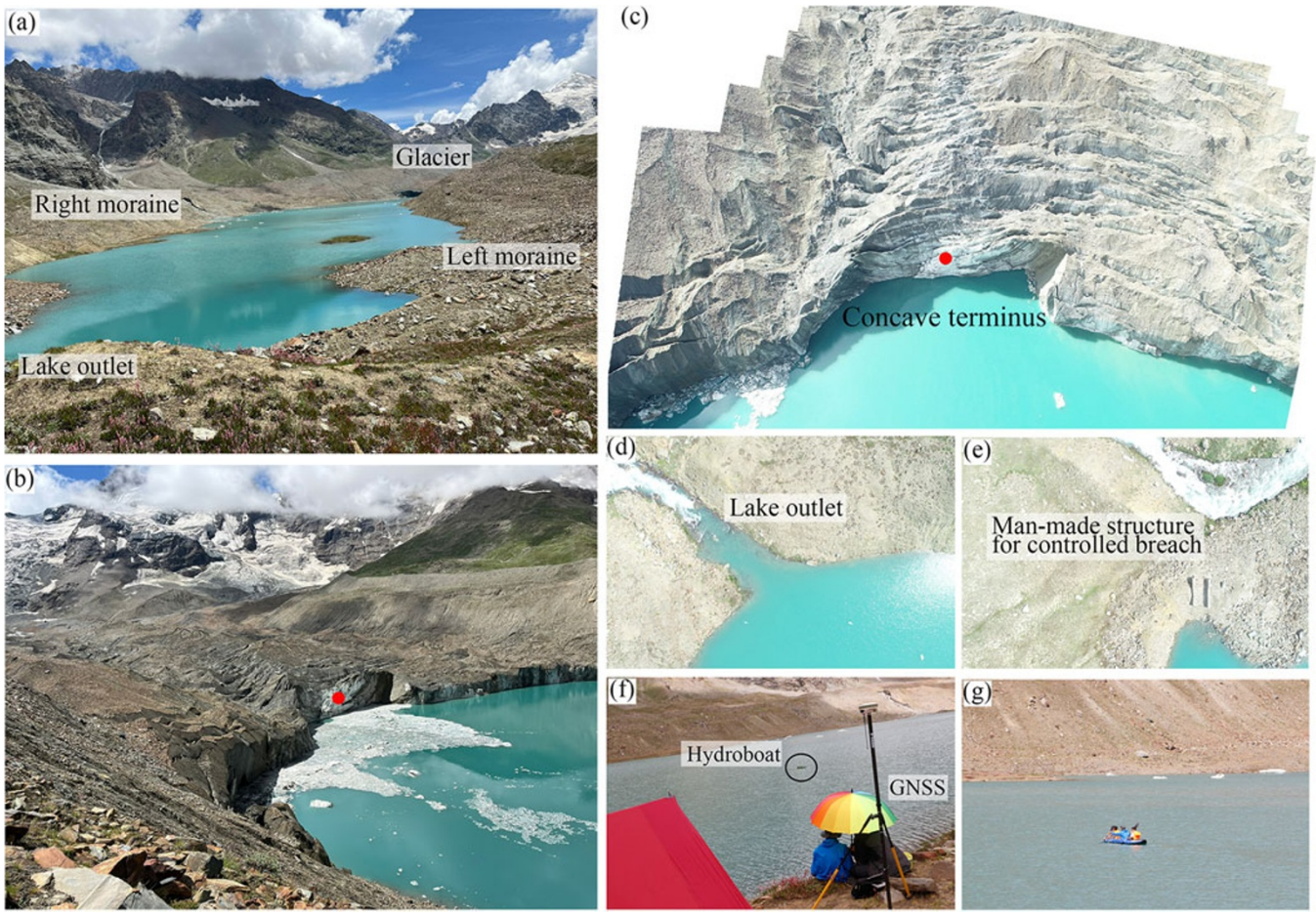

Figure 4. Field photographs of Gepang Gath Lake (GGL). (a) GGL as of August 2024. View looking up the valley. Floating ice chunks are very common in GGL. The water of GGL is sediment-free. Both sides of the lake are characterised by a lateral moraine ridge, which acts as a 'gutter' and prevents landslides on the lake from steep valley sides. (b) Close-up view of the terminus from the right lateral moraine. (c) The concave terminus shape depicts the fast retreat of the glacier. Calving is a very frequent event in GGL. (d) Lake outlet as of 7th August 2024, approx. 6 m wide. (e) A man-made structure is located on the left side of the outlet. The height difference between the lake water level and the structure is approx. 5 m. (f) GNSS base station and hydroboat survey at GGL. (g) Kayaking on GGL for manual depth measurements.

Since its formation from a small moraine-dammed lake in the 1970s, GGL has experienced substantial growth (Patel and others, 2017; Kumar and others, 2021; Das and others, 2024). The retreat of the Gepang Gath Glacier has directly facilitated the lake's expansion (Fig. S3), with its surface area increasing from 0.15 km^2 in 1971 to 1.04 km^2 in 2024 (Text S1; Tables S3–S5; Fig. S5), corresponding to an average annual growth rate of 0.02 km^2 a^{-1}. The lake's length has expanded from 580 m in 1971 to 2482 m in 2024, reflecting an average growth rate of ~36 m a^{-1} (Tables S3–S5). Several studies (Allen and others, 2016; Prakash and Nagarajan, 2017; Das and others, 2024) have categorised GGL as vulnerable to future GLOFs. The lake drains via Sissu Nalla, which joins the Chandra River ~11 km downstream. Given its upstream location from Sissu village—a settlement that has experienced significant expansion in recent years—GGL presents notable hazard implications.

2.4. Samudra Tapu Lake

The STL is located at an elevation of 4156 m asl and is fed by the Samudra Tapu Glacier, the second-largest glacier in the Chandra Basin (Table 1). The lake is surrounded by steep mountain slopes composed of unconsolidated sediments (Fig. 5a). As of August 2024, STL measured 2.35 km in length and had a maximum width of 870 m (Tables S3–S5). Geomorphologically, STL is situated on an outwash plain and is impounded by low-gradient moraine deposits (Fig. 5b). The lake's moraine is primarily composed of stratified sand and gravel, indicative of glaciofluvial deposition (Fig. 5b). STL is characterized by high turbidity, with substantial amounts of suspended sediment in the water (Fig. 5c).

Over the past five decades (1971–2024), STL has expanded from 0.24 km^2 to 1.63 km^2 in surface area (Text S1; Tables S3–S5; Figs S4–S5). The expansion of STL has been more pronounced (~0.03 km^2 a^{-1}) than other studied lakes (Fig. S5). Previous studies (Allen and others, 2016; Rao and others, 2023; Das and others, 2024) categorised STL as one of the potentially dangerous glacial lakes in the western Himalayas.

3. Data and methods

3.1. In-situ bathymetry survey

USV-based bathymetric surveys were conducted for three glacial lakes (KTL, GGL, STL) in August 2024, while a kayak-based survey was carried out for PNL in August 2022. All surveys were conducted during the ablation season (i.e. August) to minimise

Figure 5. Field photographs of Samudra Tapu Lake (STL). (a) Valley morphology of Samudra Tapu Glacier. STL is situated on the outwash plain depressions. Lake water is blocked by the small sediment ridges. The outlet is approx. 10 m wide. (b) Close-up view of the lake outlet showing the glaciofluvial deposit types. (c) View looking towards the up valley. The water of STL is highly turbid as compared to GGL. (d) Water ice interaction of STL. The frontal ice face has approx. free board of 23 m as of 17 August 2024. (d) Water-ice interaction near the valley edges of the right side of the terminus. Blue, white and red circles indicate the location of the zoomed panel.

the presence of floating ice chunks on the water surface. Figure 6 provides a schematic overview of the methodology used for bathymetric data acquisition and processing.

3.1.1. USV-based survey

A USV system (Satlab Hydroboat 1100 model) was used for this study. It comprises of four core modules: power, telemetry, navigation and data acquisition (Fig. 7a). The vessel is equipped with a lithium-ion battery powering dual propellers, offering up to ∼ 3 hours of endurance. Remote communication between the USV, controller and laptop is maintained via a telemetry system with a range of ∼ 1.5 km. Navigation is supported by a Real-Time Kinematic (RTK)-enabled Global Navigation Satellite System (GNSS) receiver (SL900), providing centimeter-level positional accuracy and is integrated with Hydral GCS software for real-time route tracking (Fig. 7b). Depth data were recorded using a 200 kHz single-beam echo sounder with a beam angle of 5°, operating in auto mode to dynamically adjust power, gain and threshold in response to depth conditions. This allowed improved echo returns and reduced noise across variable bathymetric profiles. A fixed sound velocity of 1480 m s^{-1}, calibrated for 0°C water, and a boat draft of 0.1 m were used for accurate depth estimation. Technical specifications and system parameters of USV are detailed in Table 2.

Each lake survey was customised based on site-specific conditions such as lake size, depth and the presence of floating ice chunks to ensure optimal coverage and data quality. Bathymetric data were collected along a predefined grid of longitudinal and transverse transects and monitored in real time during the survey. Minor deviations from planned transects were made as needed to safely navigate around large icebergs while maintaining continuous data collection. Surveys were conducted during early morning hours to minimise wind-induced disturbances. Multiple GNSS base stations were strategically (i.e. maximising uninterrupted visibility and line-of-sight communication between the USV and the GNSS base station) placed along the lake edges, depending on lake length and terrain accessibility, to support accurate positioning. In floating ice-dominated sections of GGL (see Fig. 4b), we employed a hybrid method where the USV was tethered to a kayak and manually manoeuvred through dense ice patches. This ensured safe navigation without compromising sonar data collection (see Section 5.3 for operational challenges). This method

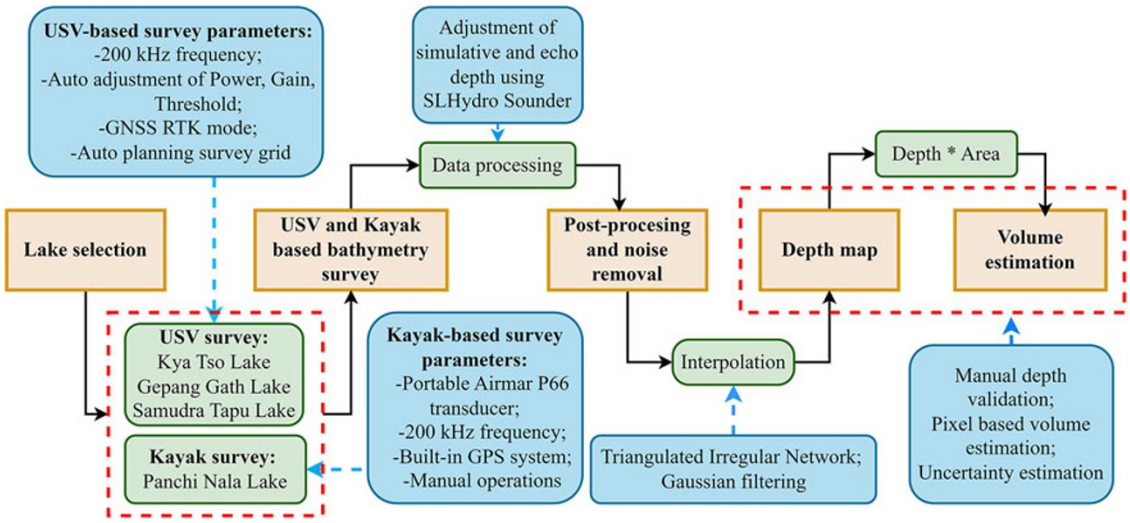

Figure 6. Flowchart of methodology used in this study.

was tested beforehand in controlled environments—at Powai Lake (19.12769°N, 72.90451°E), located adjacent to the Indian Institute of Technology Bombay (IITB) campus, and in the IITB campus swimming pool—to ensure operational feasibility. Supplementary equipment (i.e. inflatable kayak, rope, rugged laptop) and field strategies were employed as needed. The USV recorded depth data at one-second intervals throughout each of the surveys. The total survey distances recorded were 4.44 km for KTL, 28.51 km for GGL and 18.24 km for STL.

3.1.2. Kayak-based survey

We conducted the depth survey of PNL using a portable echo sounder mounted on an inflatable kayak. The hydrographic setup included a Catable Sea Eagle 380x Explorer kayak, an Airmar P66 single-beam transducer and a Simrad GO5 XSE fishfinder console (Table 3). The system recorded depth, geographic coordinates and timestamps through the Simrad's built-in GPS interface. The complete survey kit also included safety and utility equipment such as paddles, life jackets, a 12 V battery, a rope with lead weight and a measuring tape. Ramsankaran and others (2023) demonstrated the capabilities of kayak-based survey procedure at high-altitude lakes in the western Himalaya. Technical specifications of the kayak-based system adopted in this study are summarised in Table 3.

Based on the lake characteristics and morphology (see Fig. 3), the depth of the PNL was expected to be shallow, and therefore, the transducer was operated at a frequency of 200 kHz. The transducer was positioned at the side of the kayak with its face towards the forward direction of the movement. It was ensured that the transducer remained at a depth of 10 cm from the water surface while surveying to avoid errors due to air traps. Locations near large chunks of mud and rocks, as well as shallow depths of <1 m, were avoided during the survey to avert any possible collision and aground, which may cause damage to the kayak and the echo sounder. The Airmar P66 echo sounder collected depth points at approximately 1-m spatial intervals.

3.1.3. Manual depth measurements for validation

The bathymetry data recorded by the echo sounder were collected in continuous mode (Fig. 7c), while validation was carried out in waypoint mode. Manual depth measurements were performed at selected locations in GGL and STL to validate the echo sounder data. These validation points were primarily chosen in the shallower zones of the lakes to increase confidence in measurement accuracy. Depth was measured using a dead weight attached to a rope and a measuring tape. During the process, extra care was taken to ensure that the rope remained taut and vertical underwater, ensuring reliable depth readings. A total of six and 10 points were measured at GGL and STL, respectively, for cross-comparison with echo sounder depth data.

3.2. Bathymetry data processing and volume estimation

During post-processing, several noise artefacts were identified in the echogram, particularly in areas where the simulated depth (red line) and the digital echo signal (blue line) in the SLHydro Sounder interface did not align (Fig. 7c). The digital depth represents the raw signal derived from the echo sounder, based on the time taken for the sonar pulse to return from the lakebed. In contrast, the simulative depth is a modelled curve generated by the software, which applies bottom-detection algorithms to create a best-fit line from the raw data. Accurate depth measurements are typically indicated by close agreement between the two. However, in regions with rapid depth variations or weak bottom returns, noticeable mismatches occurred (Fig. 7c), indicating signal distortion or measurement uncertainty. The primary sources of noise could be attributed to: (i) intermittent GPS signal loss, (ii) motion-induced errors—particularly in deeper areas where return echoes were delayed and (iii) variable acoustic penetration due to turbidity and salinity differences. We closely inspected the echogram profiles and made corrections where applicable to ensure dataset reliability. Final post-processed depth points were exported at 1-m intervals for interpolation. The Airmar P66 transducer provides a bathymetry file with a binary format (.sl2 extension), which was processed in the ReefMaster version 2 software package (https://reefmaster.com.au/) for depth estimation.

Final post-processed depth points are heterogeneously distributed across all studied lakes (Fig. 8). Bathymetric models were created within ReefMaster software using the TIN interpolation technique. The data points were triangulated, and interpolation

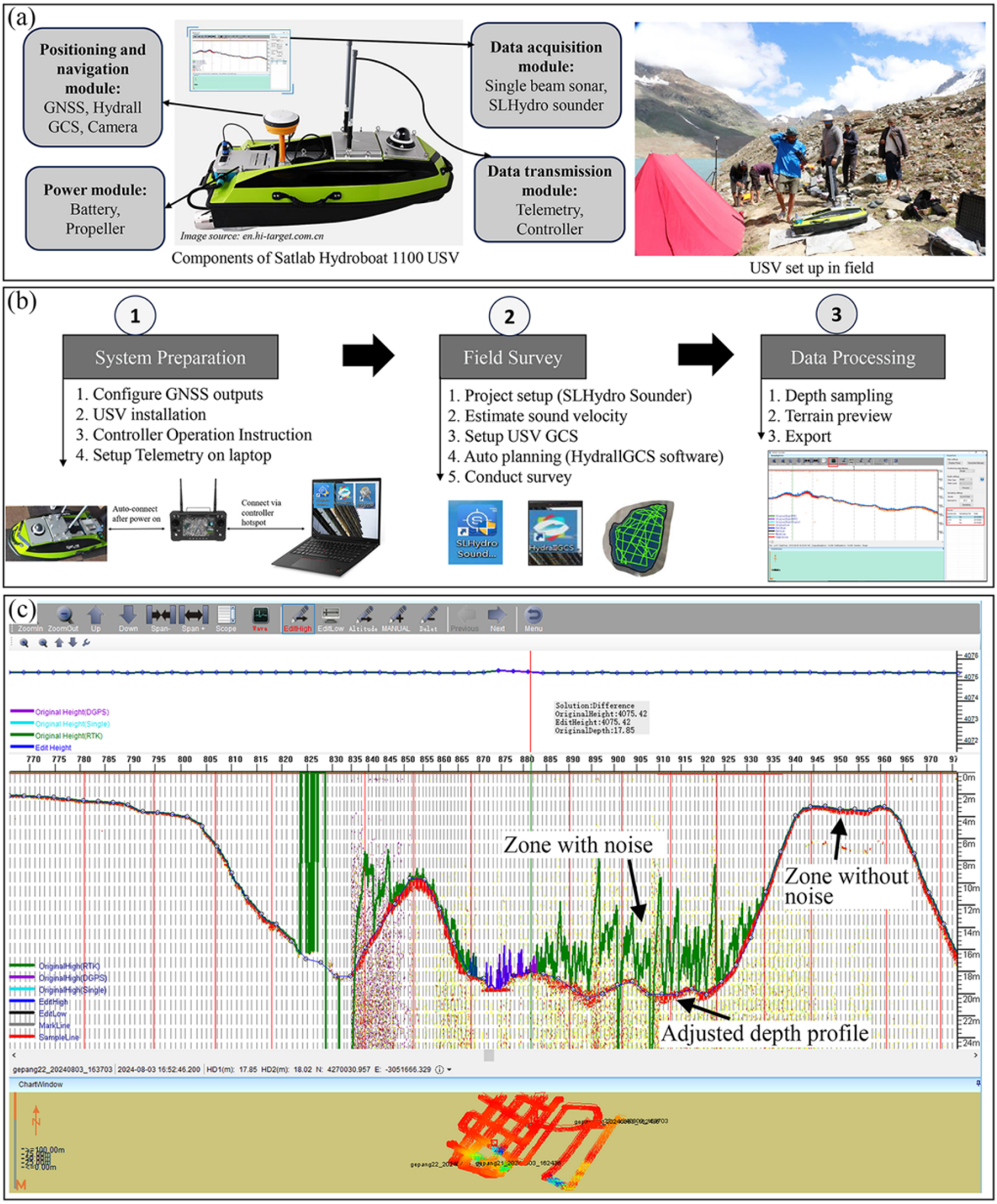

Figure 7. A USV module, data collection procedure and post-processing of depth datasets. (a) Component of the Satlab Hydroboat 1100 USV module. (b) Steps associated with the bathymetry survey and data collection. (c) An example of post-processing of echograms in SLHydro software for Gepang Gath Lake. The red line denotes the simulative echo depths, and the blue dotted line (overlaid on the red line) represents the digital echo signal received by the transducer.

between them was performed based on the slope of the connecting triangles. The interpolated values were then gridded and further refined using Gaussian smoothing. Bathymetric modelling requires a shoreline with zero depth. Since no 'zero depth' data were

Table 2. USV-based bathymetry survey specifications adopted in this study

System details	Value/Description	Remarks
USV specifications	Satlab Hydroboat 1100	High-precision hydrographic USV with a compact (135 × 56 × 34 cm), lightweight (10 kg) carbon fiber hull. IP67-rated with dual propellers, 360° camera, and veering-based steering.
Model		
Maximum speed	6 m s^{-1}	Enables efficient coverage of large lake areas.
Battery endurance	~3 hours at 2 m s^{-1} (single battery)	Varies with speed and temperature; extra battery needed for larger lakes.
Boat draft	0.1 m	Allows safe operation in shallow water zones.
USV controller and GNSS system		
System	Android	User-friendly control system with touchscreen interface.
Software	Hydral GCS	Supports mission planning and real-time USV navigation.
Control range	~1.3 km on 2.4 GHz	Limited by wireless transmission range.
GNSS receiver	SL900 RTK-GNSS	Provides high-precision geolocation; characterised by National Marine Electronics Association (NMEA − 0183) type with a baud rate of 19200 and a 5 Hz frequency.
Satellite compatibility	GPS, Baidu, GLONASS, Galileo	Multi-constellation support improves signal stability.
RTK accuracy	Horizontal: ± 8 mm + 1 ppm RMS vertical: ± 15 mm + 1 ppm RMS	Ensures sub-decimeter precision for depth georeferencing.
Echo sounder and acoustic system		
Sonar system	Single-beam echo sounder	Standard method for depth profiling.
Depth range	0.15 m—200 m	Suitable for both shallow and deep lakes.
Accuracy	±0.01 m + 0.1% × Depth	High accuracy for precise bathymetric mapping.
Frequency	200 kHz	Optimised for shallow-water surveys to reduce bottom interference.
Beam angle	5° ± 0.5°	Narrow beam ensures higher resolution.
Sound speed	1480 m s^{-1}	Calibrated for cold glacial lake water.
Survey mode	Auto adjustment	Auto power, gain, and threshold adjustment optimise echo sounder performance by dynamically tuning signal strength, sensitivity, and noise filtering based on water depth and conditions.
Software and post-processing		
User VCOM	Port connection	Facilitates communication between USV and the computer.
Hydral GCS	Mission planning	Enables pre-programmed and real-time navigation.
SLHydro Sounder	Bathymetric data acquisition, processing, correction, export	Provides comprehensive depth data handling capabilities.

Table 3. Kayak-based bathymetry survey specifications adopted in this study

System details	Value/Description	Remarks
Kayak model	Catable Sea Eagle 380x Explorer	Sea Eagle 380x measures 380 cm × 90 cm, has a hull weight of 18 kg, and offers an estimated cruising speed of 3 − 6 km/h.
Portable echo sounder	Airmar single-beam P66 transducer	Developed by Airmar Technology Corporation (USA), weighs ~ 0.5 kg and operates at 50 kHz and 200 kHz.
Controller	Simrad GO5 XSE Fishfinder console	Simrad GO5 XSE is a compact, 5-inch colour touchscreen chart plotter and fishfinder, ideal for cruising and fishing. It supports sonar and sounder functionalities, is compatible with C-Map US Coastal/Inland charts, features a high-resolution (480 × 800) horizontal display, and operates at 13.5 V DC.
Frequency used	200 kHz	Shallow depth of the lake.
GPS receiver	Built-in GPS	Simrad GO5 XSE is equipped with a built-in 10 Hz GPS receiver that offers ~ 3 m positional accuracy.
Additional equipment	Life jackets, 12 V battery, paddles	Necessary to safely operate the kayak.

collected from the outline extent of the lakes, we generated lake extents using multispectral PlanetScope imagery acquired closest to the survey dates (see supplementary Text S1 for details). Points were generated at 1-m intervals along the derived lake boundary polylines and assigned depths of zero. These points were appended onto the validated lake bathymetric points to complete the sounding databases for bathymetric modelling. Zero depth points were removed at the glacier calving front to avoid forcing the interpolated bathymetry to zero (Yao and others, 2012; Haritashya and others, 2018; Li and others, 2021). This was required since the TIN method does not interpolate outside the convex hull and therefore would not otherwise interpolate bathymetry to the calving front.

Depth maps were generated on a 1-m resolution grid and georeferenced to the WGS 84 ellipsoid. Lake volume was then estimated by integrating depth values across the mapped area, using the following equation:

$$V = \sum_{i=1}^{n} D_i * P \quad (1)$$

where V is the volume (m^3); D_i is the depth (m) at the i-th pixel; n is the number of pixels in the lake area; P is the pixel size (m^2) of the bathymetric map.

3.3. Uncertainty analysis

We estimated volume uncertainty by aggregating depth uncertainty from different sources. Following Haritashya and others (2018), we quantified depth uncertainty using water

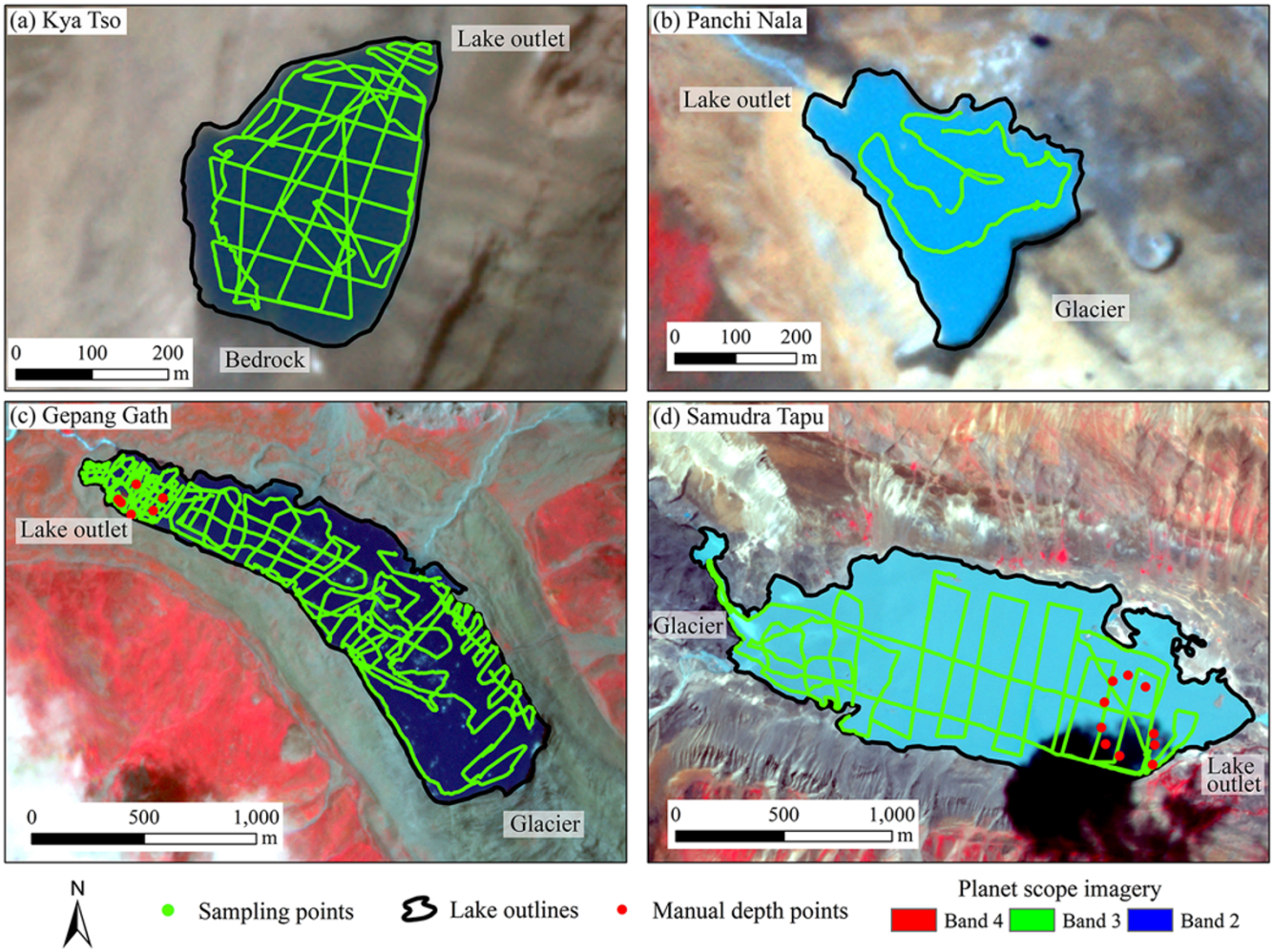

Figure 8. Sampling points of the USV for investigated lakes in the western Himalayas (background image: PlanetScope RGB): (a) Kya Tso Lake, (b) Panchi Nala Lake, (c) Gepang Gath Lake, and (d) Samudra Tapu Lake.

depth-normalised 2-σ (standard deviation). To assess this uncertainty, we randomly selected > 10 000 points distributed along and across all surveyed lakes. We validated the interpolated bathymetry depth by comparing it with depths obtained from the echo sounder. The overall (i.e. mean) depth uncertainty (2-σ) was found to be ∼1.5%. Additionally, the echo sounder data accuracy is suggested to be 0.01 m (± 0.1%) of depth. The sound velocity variations due to water temperature change have relatively high uncertainty, as temperature likely varies between 0°C and 4°C in the glacial lake, as reported for several proglacial lakes in the central Himalayan region (Chikita and others, 2000; Haritashya and others, 2018). Moreover, for ± 2°C temperature uncertainty, the corresponding depth error is about ± 0.7% (e.g. about ± 0.2 m for a 30-m water depth) was considered, as proposed by Haritashya and others (2018). We excluded very small refraction-induced positional errors from error analysis for near-nadir projecting sound transmission through a single beam sonar system (i.e. Satlab 1100 hydroboat USV model). Our overall uncertainty for volume analysis was ± 2.3%. However, we acknowledge that the overall volume uncertainty may be underestimated, particularly in zones located farther from the actual survey tracks, where interpolated values contribute more significantly. This limitation is inherent in spatial interpolation and is more pronounced in areas with sparser data density.

4. Results

4.1. Comparison of manual and interpolated depths

The manual measurement points did not directly align with the Hydroboat survey path (Fig. 8c and d), so the comparison was made between the manually recorded depths and the interpolated depths derived from the echo sounder data (Table 4). The depth values recorded by the echo sounder showed good agreement with the manual measurements (Table 4). Manual depths ranged from 2.75 m to 15.11 m, with depth differences generally <0.5 m (Table 4). These differences may be attributed to wind conditions during manual measurements, which could have caused the lead-weighted rope to drift slightly, measuring a slant height rather than the true vertical depth. Although we selected areas with a high density of echo sounder data for manual measurements (see Fig. 8c and d), the interpolation process may still introduce minor deviations from the actual depth.

4.2. Bathymetry and lake volume

4.2.1. Kya Tso Lake

Based on the TIN data, the lake bathymetry of KTL was modelled as shown in Figure 9a. The KTL profile exhibits an oval shape

Table 4. Manual depth measurements at various locations of the Gepang Gath and Samudra Tapu lakes

Point ID	Lat (°N)	Long (°E)	Depth (m)		Difference (m)	Error (%)[a]
			Interpolated	Manual		
Gepang Gath Lake						
mm-gg–1	32.52835	77.21067	4.75	4.93	−0.18	−3.65
mm-gg–2	32.58839	77.21019	8.34	8.25	0.09	1.09
mm-gg–3	32.52896	77.21007	3.82	3.93	−0.11	−2.89
mm-gg–4	32.52953	77.21094	1.73	1.72	0.03	1.76
mm-gg–5	32.52898	77.21220	1.39	1.41	−0.01	−0.71
mm-gg–6	32.52849	77.21172	15.38	14.92	0.46	3.01
Samudra Tapu Lake						
st-m–1	32.49446	77.55381	1.08	1.09	−0.01	−0.92
st-m–2	32.49528	77.55394	1.58	1.92	−0.34	−17.90
st-m–3	32.49575	77.55391	4.49	4.61	−0.11	−2.32
st-m–4	32.49771	77.55356	5.03	4.72	0.31	6.57
st-m–5	32.49821	77.55271	10.05	10.25	−0.20	−1.95
st-m–6	32.49798	77.55196	14.61	14.85	−0.24	−1.61
st-m–7	32.49711	77.55152	6.68	7.15	−0.47	−7.06
st-m–8	32.49606	77.55134	3.33	3.18	0.38	4.71
st-m–9	32.49536	77.55153	4.32	4.45	−0.13	−2.92
st-m–10	32.49486	77.55219	1.62	1.64	−0.02	−1.22

[a]Error = (Sonar − Manual survey)/Manual survey × 100%.

(Fig. 9a). The basin bottom of the lake is relatively flat, while its flanks are steep, with slopes ranging from 60° to 70°. The right side is steeper than the left (Fig. 9a). From the water depth profile, it is observed that the depth gradually increases from the moraine dam to the centre of the lake and then gradually decreases towards the lake inlet (Fig. 10a). The depth changes from the lowest (0.24 m) to the highest (15.76 m) over a distance of 270 m from the lake outlet (Fig. 10a). Since KTL is detached from the parent glacier, changes in depth are represented as a linear decrease towards the lake inlet, assuming zero water depth at the lake boundary. On August 2024, KTL had a surface area of 0.09 km^2, with a maximum depth of 15.76 m and an average depth of ∼9 m (Table 1). The volume of KTL was estimated to be $0.89 \pm 0.02 \times 10^6$ m^3.

4.2.2. Panchi Nala Lake

The bathymetric profile of PNL shows a gradual deepening from the moraine-dammed outlet towards the glacier terminus (Fig. 9b). The lake bottom is relatively undulated, characterized by multiple small depressions and sediment mounds, which were also observed during field surveys (see Fig. 3). Along the longitudinal profile, the depth increases from 0.12 m to 2.23 m within the first 100 m from the lake outlet. Between 220 m and 350 m, the depth exhibits a steep increase from 4.23 m to 10.43 m (Fig. 10b). Near the glacier snout (i.e. 350–450 m along the longitudinal profile), the average depth remains ∼10 m (Fig. 10b). This pattern reflects the characteristic up-valley deepening of a glacially eroded basin. On August 2024, PNL had a surface area of 0.11 km^2, with a maximum depth of 10.52 m and an average depth of 4.25 m (Table 1). The lake's volume was estimated at $0.44 \pm 0.02 \times 10^6$ m^3.

4.2.3. Gepang Gath Lake

GGL bed morphology is characterized by a gently sloping (deepening) bed from the lake outlet to the mid-point, followed by a slightly steeper decline towards the lake-glacier boundary (Fig. 9c). The deepest part of the trough is located closer to the calving front. Such up-valley deepening is common in glacial valley systems, as similar has been reported for central Himalayan lakes (Haritashya and others, 2018). Most of the central section of the lake (800–1500 m) along the longitudinal transect shows depths between 20 m and 40 m, with a steep gradient of >40° (Fig. 10c). Between 1500 m and 2500 m along the longitudinal profile, lake bed is flat, characterised by three small circular troughs with depth >45 m (Fig. 10c). The maximum and average depth of GGL are 46.34 m and 22.46 m, respectively, and it contains $24.26 \pm 0.4 \times 10^6$ m^3 of water as of August 2024 (Table 1).

4.2.4 Samudra Tapu Lake

STL is the biggest and deepest of the four lakes studied here (Fig. 9d). STL's bottom profile ranges from 0.01 m around the lake outlet to as much as ∼59 m deep near glacier terminus (Figs. 9d and 10d), characterised by heterogeneous mounds and depressions along long profile (Fig. 10d). Going up valley, the lake bottom gradually increases, maximum depth inclined mostly towards left flank (Fig. 9d). Most of the central section of the lake along the longitudinal transect shows depths between 20 m and 30 m, and locally reduces up to 15 m, which reflects a different lake bottom morphology compared to the GGL (Figs. 10c and d). The deepest section of the lake appears as a narrow 180-m long longitudinal trough located ∼100 m down valley from the glacier terminus (Figs. 9d and 10d). The central section of STL does not show a gradual deepening towards the glacier terminus as at GGL. Rather, in our interpolated bathymetric map, the bed appears undulating, characterized by several major trough areas (Fig. 10d), but the deepest points are located near the glacier terminus, like GGL and PNL. STL has a maximum and average depth of 58.65 m and 15 m, respectively, and it contains $24.69 \pm 0.4 \times 10^6$ m^3 of water in 2024, which makes STL both ∼27% deeper and ∼2% volumetrically larger than GGL (Table 1). Interestingly, the average depth of STL is ∼33% less than GGL.

5. Discussion

5.1. Comparison of in-situ volumes with other Himalayan lakes

No prior bathymetry survey of the studied lakes exists. Based on the previous studies (Prakash and Nagarajan, 2017; Das and others, 2024), we classified KTL and PNL as small lakes (size < 0.1 km^2), while GGL and STL were categorised as fast-growing large lakes (size > 1 km^2) in the western Himalayan region. Considering the size, growing pattern, and associated GLOF potentiality, we compared the depth and volume of GGL and STL with other in-situ bathymetry-derived depths and volumes to understand the

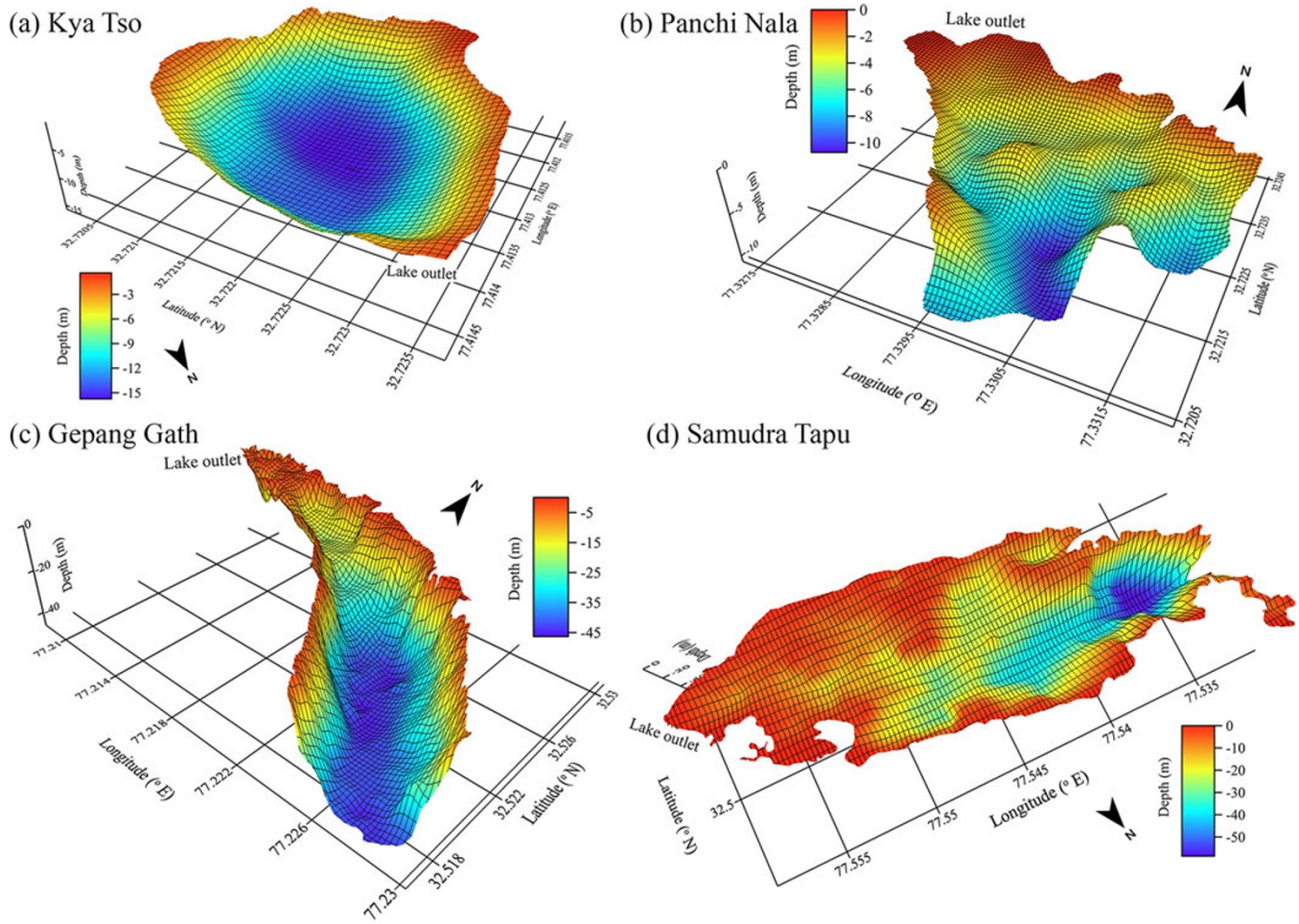

Figure 9. Basin morphology of the studied glacial lakes: (a) Kya Tso Lake, (b) Panchi Nala Lake, (c) Gepang Gath Lake, and (d) Samudra Tapu Lake.

regional trend of lake evolution across the Himalayas (Table S1). For comparisons with the present findings, we compiled the depth and volume information of other glacial lakes for which the in-situ bathymetry data are available in the Himalayan region (Fig. 11; Table S1). Bathymetry data are currently available for a small number of glacial lakes in the Himalayas, which are mainly concentrated in central Nepal, Bhutan and several basins of Tibet (Table S1). Based on the bathymetry data from the USV, we obtained the maximum and average depths of GGL of ~46 and ~22 m, respectively, in August 2024, with a lake volume of ~24.26 ± 0.41 × 10^6 m^3. STL showed maximum and average depths of ~59 and ~15 m, respectively, in August 2024, and it contains ~24.69 ± 0.42 × 10^6 m^3. In August 2024, GGL and STL had surface areas of 1.07 km^2 and 1.63 km^2, respectively, with corresponding lengths of 2.48 km and 2.43 km.

Based on in-situ bathymetric data, Duan and others (2023) reported maximum and average depths as 181 m and 85.41 m, respectively, with a total lake volume of ~102 × 10^6 m^3 for Bienong Co (1.15 km^2 in size), a moraine-dammed glacial lake in southeastern Tibet in August 2020 (Fig. 11). Similarly, Longbasaba Lake, another moraine-dammed glacial lake located in the headwaters of the Pumqu River on the northern slope of the central-eastern Himalayas, had a surface area of 1.22 km^2 in 2009, a maximum depth of 102 m, and a volume of 64 × 10^6 m^3 (Yao and others, 2012). Despite having a comparable surface area, GGL's volume is significantly lower, ~76% less than Bienong Co and ~62% less than Longbasaba Lake. In contrast, STL has a larger surface area, ~41% and ~34% greater than Bienong Co and Longbasaba Lake, respectively, yet holds only ~25% and ~16% of their total volumes. Lugge Glacial Lake in Bhutan had an area of ~1.17 km^2 in 2004, with a maximum depth of 126 m, and a volume of 58 × 10^6 m^3 (Yamada, 2004). The area of Lugge Glacial Lake is lower than that of STL, but the maximum depths and volume are much higher than the corresponding values of STL. At the time of the bathymetry survey, South Lhonak Lake in India and Imja Lake in Nepal had a similar surface area of ~1.3 km^2 (Haritashya and others, 2018; Sharma and others, 2018), which is ~20% larger than GGL and ~25% smaller than STL. In 2016, South Lhonak Lake had a maximum depth of 131 m and a total volume of 66 × 10^6 m^3 (Fig. 11). In 2014, Imja Lake had a maximum depth of 150 m and a volume of 78 × 10^6 m^3 (Fig. 11). Our analysis revealed that the volumes of both GGL and STL are ~63% and ~68% smaller than those of South Lhonak and Imja Lakes, respectively. The areas of Raphsthren Glacial Lake in Bhutan and Tsho Rolpa Glacial Lake in Nepal were 1.4 km^2 and 1.5 km^2, respectively (Fig. 11; Table S1), at the time their bathymetries were conducted (Geological Survey of India, 1995; ICIMOD, 2011). These areas are 14% and 8% smaller than that of STL. However, their volumes are significantly larger, being 171% and 252% higher than that of STL, respectively. In 2015, Lower

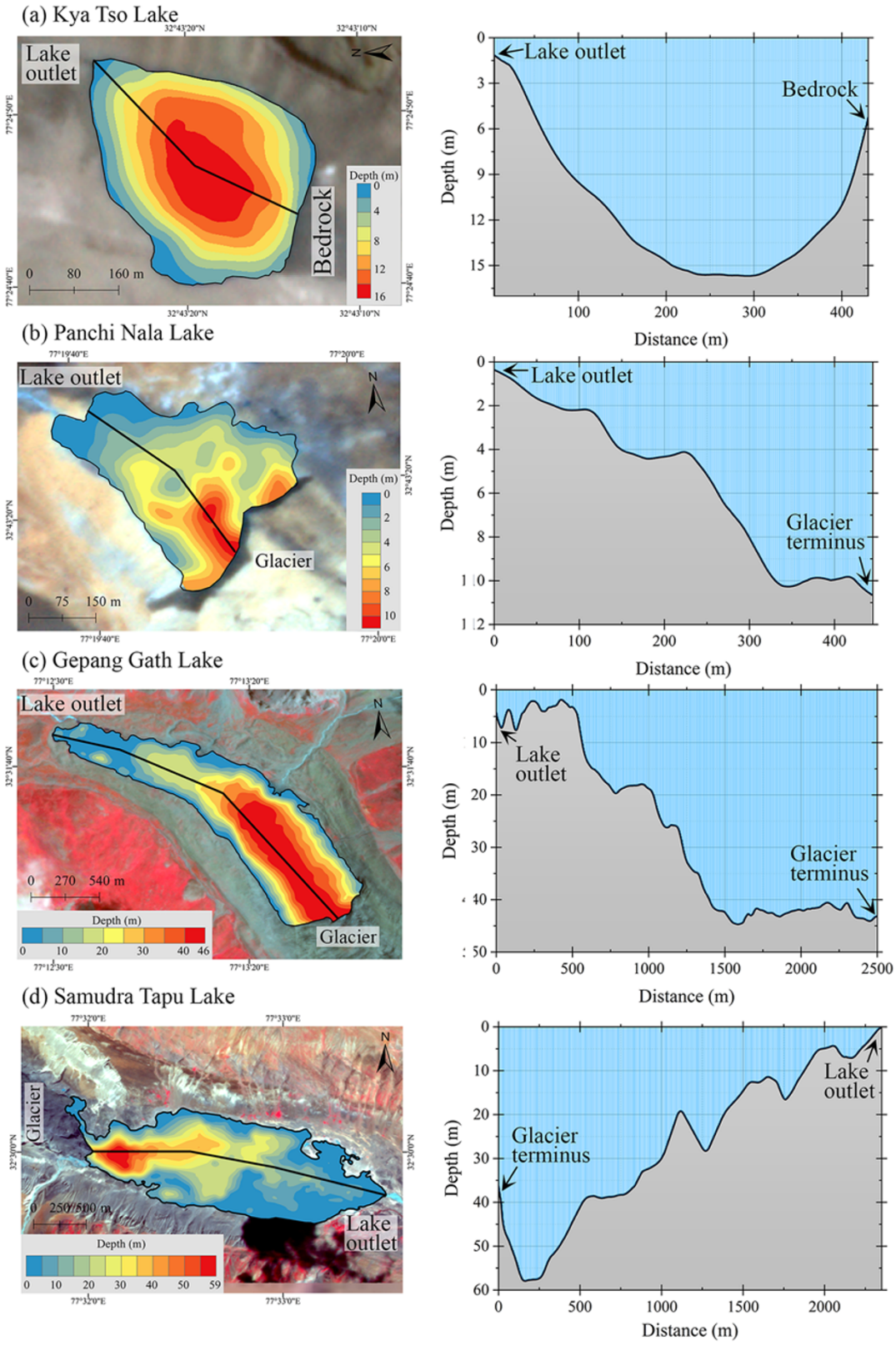

Figure 10. Bathymetric map (right panel) and water depth profile (left panel) of the studied lakes: (a) Kya Tso Lake, (b) Panchi Nala Lake, (c) Gepang Gath Lake, and (d) Samudra Tapu Lake. The depth profiles were generated along the central axis of each lake, as indicated by the black lines on the maps.

Barun Lake had a surface area of 1.8 km^2, a maximum depth of 205 m and a volume of 112×10^6 m^3 (Fig. 11). Despite having only 9% more surface area than STL, Lower Barun Lake is 247% deeper and 353% larger in volume than STL. Several other lakes across

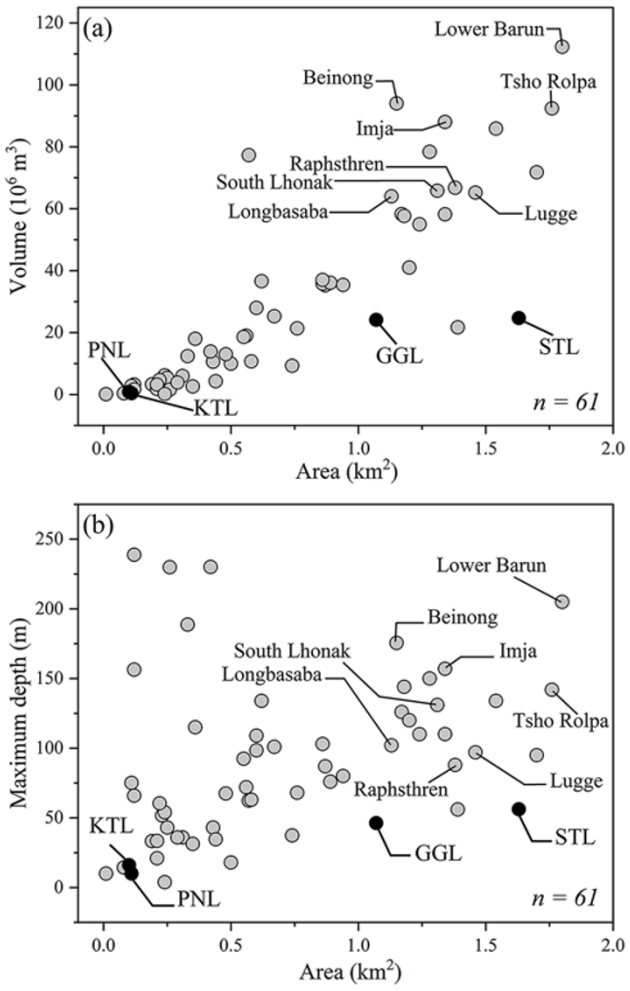

Figure 11. Distribution of (a) area-volume and (b) area-maximum depth of glacial lakes based on in-situ bathymetry across the Himalayas. Selected lakes mentioned in the discussion section are labelled for reference. The lakes investigated in this study are marked with black circles. Detailed information on 61 glacial lakes is provided in Supplementary Table S1. Abbreviations: KTL – Kya Tso Lake; PNL – Panchi Nala Lake; GGL – Gepang Gath Lake; STL – Samudra Tapu Lake.

the Himalayas show heterogeneous depth and volumetric storage, despite having comparable surface area (Fig. 11; Table S1).

Heterogeneity in volumetric storage could be attributed to variable depth, lake basin morphology, overdeepening of glacial beds, moraine height and sediment deposition patterns. Glaciation style is a key factor driving heterogeneous lake evolution in alpine environments. For instance, large lakes associated with long valley glaciers often exhibit greater depths compared to smaller lakes linked to steeper, shorter glaciers (Richardson and Reynolds, 2000). Glacial lakes typically form in irregular depressions (i.e. overdeepenings) carved by glacial activity (Haeberli and others, 2016). Variations in basin shape, slope and depth result in volume heterogeneity, even among lakes with comparable surface areas (Carrivick and Tweed, 2013; Linsbauer and others, 2016). Haritashya and others (2018) reported similar observations of four glacial lakes in the Nepal Himalayas. Zhang and others (2023c) reported variability in the volumetric assessment of 16 pro-glacial lakes in the eastern Himalayas. Subglacial drainage channels, buried ice, ice-ramps near the glacier-lake boundary (Haeberli and others, 2016) or sediment layers can further alter a lake's effective water-holding capacity (Cook and Quincey, 2015; Steffen and others, 2022). Additionally, lakes receiving high sediment loads (from erosion, avalanches or glacial flour) may experience reduced volumes due to infilling (Hardmeier and others, 2024), despite stable surface areas. For example, the highly turbid waters of STL indicate significant sediment production, likely contributing to bed deposition and infilling, in contrast to the relatively sediment-free GGL.

5.2. Comparison of volumes between in-situ bathymetry and empirical volume-area estimates

Due to the scarcity of glacial lake bathymetry data and its critical importance for glacial lake hazard assessments, researchers have developed VA empirical relationships to estimate lake volume using parameters such as surface area, width and length (Fig. 12 and references therein). In this study, we applied 20 published VA empirical equations—derived from datasets spanning global and Himalayan regions—to estimate the volumes of the studied glacial lakes (Fig. 12). These equations were previously compiled based on lake morphological types, with varying sample sizes used in their derivation (Table S2).

The results indicate that none of the empirical equations agreed with in situ bathymetry-derived volumes (Fig. 12; Table S2). Substantial discrepancies (±32–1736%) were observed between volumes estimated using existing equations and those measured via in-situ bathymetry across all four lakes. For example, applying the formula proposed by Huggel and others (Huggel and others, 2002), deviations of 47%, 240%, 57% and 180% were observed for KTL, PNL, GGL and STL, respectively (Eq. 1 in Fig. 12). Similarly, the equation by Cook and Quincey (2015) yielded volumetric deviations ranging from 54% for GGL to 276% for STL (Eq. 3 in Fig. 12). Notably, all equations except that of Wang and others (2012) produced positive deviations (overestimates) in volumetric measurements (Eq. 13 in Fig. 12). Patel and others (2017), using their empirical equation (Eq. 17 in Fig. 12), reported volumes of ~27×10^6 m^3 and ~68×10^6 m^3 for GGL and STL, respectively, as of 2014. However, our in-situ measurements revealed deviations of ~112% for GGL and 336% for STL (Table S2).

Several studies have developed VA empirical relationships by adding data from specific regions (Wang and others, 2012; Loriaux and Casassa, 2013; Cook and Quincey, 2015; Zhang and others, 2023c), suggesting that regional factors may influence the predictability of lake volume. However, based on the observations from the Himalayan regions, Qi and others (2022) reported that regional differences do not consistently improve volume predictability. Cook and Quincey (2015) critically evaluated the performance of existing empirical relationships across different regions and highlighted that even lakes within the same geographic area exhibit significant variability in volume predictability. Their findings suggest that region-specific equations are not inherently more reliable than those derived from broader datasets. Instead, lake origin and morphology play a dominant role in determining volume predictability and the suitability of empirical equations for accurate forecasting (Cook and Quincey, 2015). For instance, Zhang and others (2023c) developed a Himalayan-specific equation using bathymetric data from 59 moraine-dammed lakes. Yet, our in-situ volume measurements for moraine-dammed GGL and STL reveal substantial deviations (96–247%) from their estimates (Fig. 12; Table S2).

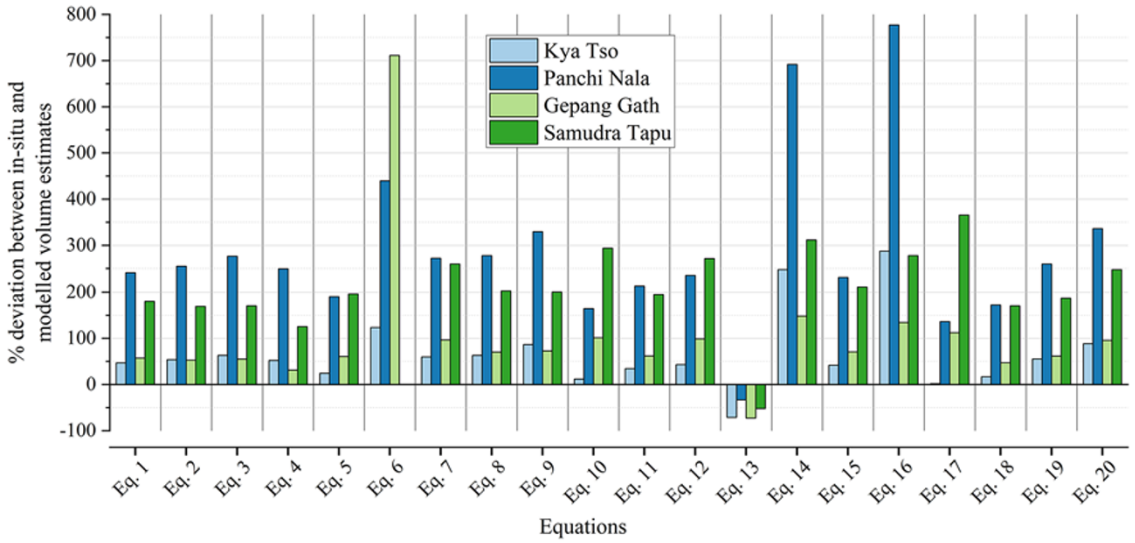

Figure 12. The percentage difference between in-situ and modelled volume estimates for the studied glacial lakes, based on 20 commonly used empirical equations. Details of each equation are provided in Supplementary Table S2. References for equations are Eq. 1: Huggel and others (2002); Eq. 2: Loriaux and Casassa (2013); Eq. 3: Cook and Quincey (2015); Eq. 4: Watson and others (2018); Eq. 5: Evans and others (1986); Eq. 6: O'Connor and others (2001); Eq. 7: Emmer and Vilímek (2014); Eq. 8, 9, and 10: Wood and others (2021); Eq. 11: Kapitsa and others (2017); Eq. 12: Sakai and others (2012); Eq. 13: Wang and others (2012); Eq. 14: Fujita and others (2013); Eq. 15: Khanal and others (2015); Eq. 16: Sharma and others (2018); Eq. 17: Patel and others (2017); Eq. 18: Miles and others (2018); Eq. 19: Watson and others (2018); Eq. 20: Zhang and others (2023c). *Note*: Data for Samudra Tapu Lake using Eq. 6 are excluded due to an unusually high deviation of 1736%.

For water volume estimation, incorrect values could provide an overestimate of potential water storage, while for risk assessment purposes, underestimates of lake volume and consequently, the possible peak discharge could be potentially dangerous (Muñoz and others, 2020; Qi and others, 2022). Since the different empirical formulas have various estimate errors for individual lakes, several studies (Cook and Quincey, 2015; Haeberli and others, 2016; Muñoz and others, 2020) have recommended the use of different approaches for lake volume estimation rather than relying on a single method.

Our study area, the upper Chenab basin, contains several potentially dangerous glacial lakes and is a GLOF-prone basin in the western Himalayas (Prakash and Nagarajan, 2017; Das and others, 2024). Previous studies have focused on glacial lake area change, volume estimation using empirical equations, and risk assessment of potentially dangerous glacial lakes in the basin (Patel and others, 2017; Prakash and Nagarajan, 2017; Kumar and others, 2021; Das and others, 2023, 2024). Due to numerous gaps in current knowledge regarding the volumes of glacial lakes in the Chenab basin, the simulation of GLOF development pathways is difficult to estimate precisely. Hence, the present study provides new datasets on in-situ bathymetry, which could be further used in future to develop a more robust VA equation for the region. Future efforts are necessary to continue and extend glacial lake bathymetric measurement programs for further volume assessment and model calibration.

5.3. Challenges and recommendations

We faced several challenges during the USV surveys. Previous studies (Haritashya and others, 2018; Muñoz and others, 2020; Li and others, 2021; Qi and others, 2022; Duan and others, 2023; Zhang and others, 2023c) have not detailed the field difficulties associated with bathymetric surveys in high-altitude regions. However, Ramsankaran and others (2023) highlighted the procedures, challenges and recommendations for conducting kayak-based surveys in Himalayan glacial lakes. Building on standard procedures, our USV-based survey methodology offers a scalable and replicable approach for bathymetric mapping in comparable glacial lake environments. Here, we outline key challenges and offer practical recommendations to enhance the efficiency and reliability of USV surveys in high-altitude glacial lake settings.

I. For this study, we deployed a Satlab Hydroboat 1100 USV equipped with a 200 kHz single-beam echo sounder with a maximum penetration capacity of 200 m. While this system is effective for lower depths (<20 m), acoustic noise emerged in higher depths (>20 m) at constant speeds due to delayed echo returns (Fig. 7c). Such challenges highlight the need for prior knowledge of tentative maximum lake depths to select appropriate transducer frequencies. Lower frequencies (i.e., 50 kHz) improve penetration in deeper areas (>10 m) but reduce resolution in shallower zones (<10 m), suggesting for use of a dual-frequency transducer (e.g., low frequency for deep areas and high frequency for shallow areas) to balance depth penetration and resolution.
II. The limited telemetry range (~1.5 km) of Satlab 1100 USV restricts real-time communication and data transmission between the boat and control system during the survey of long lakes (i.e. GGL, STL; ~2.7 km length). Several base stations are required at different locations along the lake edges, which is difficult due to steep terrain and inaccessibility. To overcome this limitation, a USV with a higher telemetry range (>5 km) is recommended for surveying large lakes (such as Imja: ~3.1 km, Lower Barun: ~2.7 km, Thulagi: ~3 km, Tso Rolpa: ~3.8 km, South Lhonak: ~2.7 km) in the Himalayas.
III. High-altitude conditions significantly reduce the USV's battery performance, limiting operational time. In our surveys, a single battery charge provided ~3 hours of runtime—insufficient to fully cover large lakes like GGL and STL, given their size and required survey line density. To address this,

we recommend carrying additional battery sets to ensure uninterrupted operations. Moreover, transporting the USV and associated equipment to remote high-altitude lake sites presents major logistical challenges. The USV's large dimensions and heavy protective cases demand considerable manpower and extended time for transport. Ensuring continuous power supply further complicates logistics, as it requires carrying a portable generator—often bulky and difficult to handle in rugged terrain. These constraints necessitate more porters and additional days in the field. To improve feasibility and efficiency in such environments, we strongly recommend using more compact, lightweight USV systems with enhanced battery capacity, which would ease transportation and reduce logistical demands.

IV. The strong winds in the glacial valley during afternoons made surveying much more difficult since these winds helped build strong water currents that caused USV to bounce during the survey. Studies reported that waves generated bouncing of USV lead to air pockets between the boat and water that scatter acoustic signals and introduce noise in echograms (Shabangu and others, 2014). It is suggested to perform the survey during the first half of the day, especially during morning hours when calm weather persists. It is because, in glaciated regions, the wind speed will be relatively higher during the afternoons, resulting in more bounce of USV, even at slow speeds.

V. The relationship between USV speed and depth of water is one of the important factors that need to be kept in mind during the survey. Using a single-beam high-frequency sounder, one needs to adjust the boat speed with varying depths. Constant boat speed during auto mode can lead to motion-induced errors and noise in echo signals, especially in deeper areas where return echoes take longer to reach the sensor. We observed similar noise in echograms during the survey at GGL, depth >30 m. It is suggested to adjust boat speed dynamically based on depth: slower speeds (<1 m s^{-1}) for deeper areas and faster speeds for shallower areas. In addition, a USV equipped with adaptive speed control algorithms is recommended to optimize the survey.

VI. Among the four lakes surveyed, STL exhibited the highest turbidity (see Fig. 5). Surveying in turbid lakes can produce additional acoustic noise due to suspended sediments scattering the echo-sounder signals (Santos and others, 2020). While we could not isolate the specific contribution of turbidity to signal scattering, any noise artefacts observed in the raw data were successfully removed during post-processing of the bathymetry datasets.

VII. During the survey, we encountered operational challenges due to large floating ice chunks in the lakes, particularly in GGL, where they were more prevalent than in the other three lakes. These ice chunks hindered the auto-mode survey plan by obstructing predefined paths, destabilizing the USV and posing risks of equipment damage. Although the USV was equipped with a 360-degree omnidirectional camera for obstacle monitoring, this proved insufficient for navigating ice-dense zones. To address this, we implemented a hybrid approach: the USV was tethered to a kayak, which was manually manoeuvred through ice-dominated areas. This strategy enabled access to otherwise inaccessible regions and conserved battery life by deactivating the USV's propellers during kayak-led navigation. For future surveys in high-altitude glacial lakes, where ice calving is a common phenomenon, we recommend USVs equipped with advanced obstacle detection and avoidance systems to enhance safety and efficiency.

High-altitude glacial lakes present unique challenges for USV-based bathymetric surveys, including environmental factors (wind, ice, turbidity) and operational limitations (battery life, telemetry range, transducer performance). Addressing these challenges requires a combination of advanced technology, adaptive survey strategies and careful planning. By implementing the recommendations above, one can improve the efficiency, accuracy and safety of USV surveys in these challenging environments.

6. Conclusions

In this study, we have modelled the basin morphology of four lakes in the western Himalayas based on an in-situ bathymetry survey. The bathymetric survey revealed significant variations in lake depths and storage capacities, with maximum depths of 16 m, 10 m, 46 m and 59 m for Kya Tso Lake, Panchi Nala Lake, Gepang Gath Lake and Samudra Tapu Lake, respectively. Their corresponding volumes were estimated at 0.89×10^6 m^3, 0.44×10^6 m^3, 24.12×10^6 m^3 and 24.69×10^6 m^3. A comparison with volume estimates from commonly used empirical equations revealed substantial discrepancies (±36–1736%), highlighting the limitations of these models in accurately predicting glacial lake volumes. The findings highlight the importance of conducting targeted in-situ bathymetric surveys, particularly for potentially dangerous glacial lakes in the region, to support more accurate hazard assessments based on lake-specific geomorphological characteristics. Future studies should focus on integrating high-resolution USV-based bathymetric data with advanced hydrodynamic modelling to improve risk assessment and mitigation strategies for GLOFs in the region.

Supplementary material. The supplementary material for this article can be found at https://doi.org/10.1017/jog.2025.10082.

Data availability statement. The in-situ bathymetry and multi-temporal lake boundary datasets can be downloaded from Zenodo at https://doi.org/10.5281/zenodo.16677319.

Acknowledgements. We would like to thank the porters for their invaluable assistance during the fieldwork. We sincerely appreciate the technical support for the USV provided by Satlab and Hi-Target. Thanks to Dr Parmanand Sharma from the National Centre for Polar and Ocean Research (NCPOR) for supporting us during the USV survey at Kya Tso and Samudra Tapu Lakes. The first author extends gratitude to Luvkesh Attri, PhD scholar at the Hydro-Remote Sensing Applications (H-RSA) group, IIT Bombay, for support during the USV survey. The authors thank Sayantan Mandal, Ajay Godara, and Navin Kumar, PhD scholars at H-RSA group, IIT Bombay, for their support during the Kayak-based survey at Panchi Nala Lake. This work was supported by the institute postdoctoral program of the Indian Institute of Technology Bombay, Mumbai and by the Science and Engineering Research Board (SERB), Department of Science and Technology (DST), Government of India for the project titled 'Modelling the evolution of large glacier-fed lakes in Western Himalayas' under Core Research Grant (CRG). We thank the Chief Editor, Dr Hester Jiskoot, the Scientific Editor, Dr David Rounce, the Associate Chief Editor, Dr Nicolas Eckert, and the two anonymous reviewers for their constructive and insightful comments, which have greatly improved the quality of the manuscript.

Author contributions. Suresh Das conducted USV surveys at KTL, GGL and STL, analysed depth data, created figures and drafted the original manuscript. RAAJ Ramsankaran performed a kayak-based survey at PNL, supervised

the study, acquired funding and contributed to writing and reviewing the manuscript.

Competing interests. The authors declare that they have no known competing financial interests or personal relationships that could have appeared to influence the work reported in this paper.

References

Allen SK, Linsbauer A, Randhawa SS, Huggel C, Rana P and Kumari A (2016) Glacial lake outburst flood risk in Himachal Pradesh, India: An integrative and anticipatory approach considering current and future threats. *Natural Hazards* **84**(3), 1741–1763. doi:10.1007/s11069-016-2511-x

Byers AC, Rounce DR, Shugar DH, Lala JM, Byers EA and Regmi D (2019) A rockfall-induced glacial lake outburst flood, Upper Barun Valley, Nepal. *Landslides* **16**(3), 533–549. doi:10.1007/s10346-018-1079-9

Carrivick JL and Tweed FS (2013) Proglacial Lakes: Character, behaviour and geological importance. *Quaternary Science Reviews* **78**, 34–52. doi:10.1016/j.quascirev.2013.07.028

Carrivick JL, Tweed FS, Sutherland JL and Mallalieu J (2020) Toward numerical modeling of interactions between ice-marginal proglacial lakes and glaciers. *Frontiers in Earth Science* **8**(October), 1–9. doi:10.3389/feart.2020.577068

Chikita K, Joshi SP, Jha J and Hasegawa H (2000) Hydrological and thermal regimes in a supra-glacial lake: Imja, Khumbu, Nepal Himalaya. *Hydrological Sciences Journal* **45**(4), 507–521. doi:10.1080/02626660009492353

Cook SJ and Quincey DJ (2015) Estimating the volume of Alpine glacial lakes. *Earth Surface Dynamics* **3**(4), 559–575. doi:10.5194/esurf-3-559-2015

Das S, Das S, Mandal ST, Sharma MC and Ramsankaran R (2024) Inventory and GLOF susceptibility of glacial lakes in Chenab basin, Western Himalaya. *Geomatics, Natural Hazards and Risk* **15**(1), 2356216. doi:10.1080/19475705.2024.2356216

Das S, Sharma MC, Murari MK, Nüsser M and Schmidt S (2023) Half-a-century (1971–2020) of glacier shrinkage and climatic variability in the Bhaga basin, western Himalaya. *Journal of Mountain Science* **20**(2), 299–324. doi:10.1007/s11629-022-7598-9

Deswal S, Sharma MC, Saini R, Dalal P and Kumar P (2020) Preliminary results of hybrid bathymetry and GLOF risk assessment for Neelkanth lake, Lahaul Himalaya, India. *Current Science* **119**(9), 1555–1557. doi:10.18520/cs/v119/i9/1555-1557

Duan H and 8 others (2023) Lake volume and potential hazards of moraine-dammed glacial lakes - A case study of Bienong Co, southeastern Tibetan Plateau. *Cryosphere* **17**(2), 591–616. doi:10.5194/tc-17-591-2023

Emmer A and Vilímek V (2014) New method for assessing the susceptibility of glacial lakes to outburst floods in the Cordillera Blanca, Peru. *Hydrology and Earth System Sciences* **18**(9), 3461–3479. doi:10.5194/hess-18-3461-2014

Evans SG (1986) The maximum discharge of outburst floods caused by the breaching of man-made and natural dams: Reply. *Canadian Geotechnical Journal* **23**(3), 385–387. doi:10.1139/t87-062

Fischer M, Korup O, Veh G and Walz A (2021) Controls of outbursts of moraine-dammed lakes in the greater Himalayan region. *Cryosphere* **15**(8), 4145–4163. doi:10.5194/tc-15-4145-2021

Fujita K and 6 others (2013) Potential flood volume of Himalayan glacial lakes. *Natural Hazards and Earth System Sciences* **13**(7), 1827–1839. doi:10.5194/nhess-13-1827-2013

Geological Survey of India (1995) Geology, environmental hazards and remedial measures of the lunana Area, Gasa Dzongkhang. Report of 1995 Indo-Bhutan Expedition. Samtse.

Haeberli W, Linsbauer A, Cochachin A, Salazar C and Fischer UH (2016) On the morphological characteristics of overdeepenings in high-mountain glacier beds. *Earth Surface Processes and Landforms* **41**(13), 1980–1990. doi:10.1002/esp.3966

Hardmeier F, Schmidheiny N, Suremann J, Lüthi M and Vieli A (2024) Evolution, sedimentation and thermal state of the emerging pro-glacial lakes at Witenwasserengletscher, Switzerland. *Earth Surface Processes and Landforms* **49**(12), 4055–4073. doi:10.1002/esp.5941

Haritashya UK and 9 others (2018) Evolution and controls of large glacial lakes in the Nepal Himalaya. *Remote Sensing* **10**(798), 1–31. doi:10.3390/rs10050798

Huggel C, Kääb A, Haeberli W, Teysseire P and Paul F (2002) Remote sensing based assessment of hazards from glacier lake outbursts: A case study in the Swiss Alps. *Canadian Geotechnical Journal* **39**(2), 316–330. doi:10.1139/t01-099

ICIMOD (2011) *Glacial Lakes and Glacial Lake Outburst Floods in Nepal*. Kathmandu, Nepal: International Centre for Integrated Mountain Development (ICIMOD), 96.

Kapitsa V, Shahgedanova M, Machguth H, Severskiy I and Medeu A (2017) Assessment of evolution and risks of glacier lake outbursts in the Djungarskiy Alatau, Central Asia, using Landsat imagery and glacier bed topography modelling. *Natural Hazards and Earth System Sciences* **17**(10), 1837–1856. doi:10.5194/nhess-17-1837-2017

Khanal NR, Hu JM and Mool P (2015) Glacial lake outburst flood risk in the Poiqu/Bhote Koshi/Sun Koshi river basin in the Central Himalayas. *Mountain Research and Development* **35**(4), 351–364. doi:10.1659/MRD-JOURNAL-D-15-00009

King O, Bhattacharya A, Bhambri R and Bolch T (2019) Glacial lakes exacerbate Himalayan glacier mass loss. *Scientific Reports* **9**(1), 1–9. doi:10.1038/s41598-019-53733-x

Kraaijenbrink PDA, Bierkens MFP, Lutz AF and Immerzeel WW (2017) Impact of a global temperature rise of 1.5 degrees Celsius on Asia's glaciers. *Nature* **549**(7671), 257–260. doi:10.1038/nature23878

Kumar V, Mehta M and Shukla T (2021) Spatially resolved estimates of glacial retreat and lake changes from Gepang Gath Glacier, Chandra Basin, Western Himalaya, India. *Journal of the Geological Society of India* **97**(5), 520–526. doi:10.1007/s12594-021-1718-y

Li D and 6 others (2021) Expansion and hazard risk assessment of glacial lake Jialong Co in the central Himalayas by using an unmanned surface vessel and remote sensing. *Science of the Total Environment* **784**, 147249. doi:10.1016/j.scitotenv.2021.147249

Linsbauer A, Frey H, Haeberli W, Machguth H, Azam MF and Allen S (2016) Modelling glacier-bed overdeepenings and possible future lakes for the glaciers in the Himalaya-Karakoram region. *Annals of Glaciology* **57**(71), 119–130. doi:10.3189/2016AoG71A627

Loriaux T and Casassa G (2013) Evolution of glacial lakes from the Northern Patagonia Icefield and terrestrial water storage in a sea-level rise context. *Global and Planetary Change* **102**, 33–40. doi:10.1016/j.gloplacha.2012.12.012

Miles ES and 8 others (2018) Glacial and geomorphic effects of a supraglacial lake drainage and outburst event, Everest region, Nepal Himalaya. *Cryosphere* **12**(12), 3891–3905. doi:10.5194/tc-12-3891-2018

Moser KA and 19 others (2019) Mountain lakes: Eyes on global environmental change. *Global and Planetary Change* **178**(April), 77–95. doi:10.1016/j.gloplacha.2019.04.001

Muñoz R, Huggel C, Frey H, Cochachin A and Haeberli W (2020) Glacial lake depth and volume estimation based on a large bathymetric dataset from the Cordillera Blanca, Peru. *Earth Surface Processes and Landforms* **45**(7), 1510–1527. doi:10.1002/esp.4826

Nie Y, Liu Q, Wang J, Zhang Y, Sheng Y and Liu S (2018) An inventory of historical glacial lake outburst floods in the Himalayas based on remote sensing observations and geomorphological analysis. *Geomorphology* **308**, 91–106. doi:10.1016/j.geomorph.2018.02.002

O'Connor JE, Hardison JH and Costa JE (2001) *Debris Flows from Failures of Neoglacial-age Moraine Dams in the Three Sisters and Mount Jefferson Wilderness Areas*. Oregon: U.S. Geological Survey.

Patel LK, Sharma P, Laluraj CM, Thamban M, Singh A and Ravindra R (2017) A geospatial analysis of Samudra Tapu and Gepang Gath glacial lakes in the Chandra Basin, Western Himalaya. *Natural Hazards* **86**(3), 1275–1290. doi:10.1007/s11069-017-2743-4

Prakash C and Nagarajan R (2017) Outburst susceptibility assessment of moraine-dammed lakes in Western Himalaya using an analytic hierarchy process. *Earth Surface Processes and Landforms* **42**(14), 2306–2321. doi:10.1002/esp.4185

Qi M and 7 others (2022) Improving the accuracy of glacial lake volume estimation: A case study in the Poiqu basin, central Himalayas. *Journal of Hydrology* **610**(May), 127973. doi:10.1016/j.jhydrol.2022.127973

Ramsankaran R, Verma P, Majeed U and Rashid I (2023) Kayak-based low-cost hydrographic surveying system: A demonstration in high altitude proglacial lake associated with Drang Drung Glacier, Zanskar Himalaya. *Journal of Earth System Science* **132**(1), 1–9. doi:10.1007/s12040-022-02021-w

Rao BS, Joshi S, Roy P, Sweta and Raju PV (2023) *GLOF Risk Assessment of Ghepang Ghat Glacial Lake in Indus River Basin*. Hyderabad, India: National Remote Sensing Centre (NRSC), Indian Space Research Organisation (ISRO, 110.

Richardson SD and Reynolds JM (2000) An overview of glacial hazards in the Himalayas. *Quaternary International* **65**(66), 31–47. doi:10.1016/S1040-6182(99)00035-X

Sakai A (2012) Glacial Lakes in the Himalayas: A Review on Formation and Expansion Processes. *Global Environmental Research* **16**(2011), 23–30.

Santos AI, Oliveira A, Carinhas D, Pinto JP, Zacarias N and Freitas MC (2020) The acoustic properties of in-situ measured suspended sediments and their implications on concurrent ADCP response – Case studies of the Portuguese inner shelf. *Marine Geology* **419**(October 2019), 106079. doi:10.1016/j.margeo.2019.106079

Sattar A and 33 others (2025) The Sikkim flood of October 2023: Drivers, causes and impacts of a multi-hazard cascade. *Science* **387**(6740), eads2659. doi:10.1126/science.ads2659

Shabangu FW, Ona E and Yemane D (2014) Measurements of acoustic attenuation at 38kHz by wind-induced air bubbles with suggested correction factors for hull-mounted transducers. *Fisheries Research* **151**, 47–56. doi:10.1016/j.fishres.2013.12.008

Sharma RK, Pradhan P, Sharma NP and Shrestha DG (2018) Remote sensing and in situ-based assessment of rapidly growing South Lhonak glacial lake in eastern Himalaya, India. *Natural Hazards* **93**(1), 393–409. doi:10.1007/s11069-018-3305-0

Shrestha F and 9 others (2023) A comprehensive and version-controlled database of glacial lake outburst floods in High Mountain Asia. *Earth System Science Data* **15**(9), 3941–3961. doi:10.5194/essd-15-3941-2023

Shugar DH and 9 others (2020) Rapid worldwide growth of glacial lakes since 1990. *Nature Climate Change* **10**(10), 939–945. doi:10.1038/s41558-020-0855-4

Steffen T, Huss M, Estermann R, Hodel E and Farinotti D (2022) Volume, evolution, and sedimentation of future glacier lakes in Switzerland over the 21st century. *Earth Surface Dynamics* **10**(4), 723–741. doi:10.5194/esurf-10-723-2022

Sutherland JL, Carrivick JL, Gandy N, Shulmeister J, Quincey DJ and Cornford SL (2020) Proglacial lakes control glacier geometry and behavior during recession. *Geophysical Research Letters* **47**(19), e2020GL088865. doi:10.1029/2020GL088865

Taylor C, Robinson TR, Dunning S, Rachel Carr J and Westoby M (2023) Glacial lake outburst floods threaten millions globally. *Nature Communications* **14**(1), 1–10. doi:10.1038/s41467-023-36033-x

Tweed FS and Carrivick JL (2015) Deglaciation and proglacial lakes. *Geology Today* **31**(3), 96–102. doi:10.1111/gto.12094

Veh G, Korup O, von Specht S, Roessner S and Walz A (2019) Unchanged frequency of moraine-dammed glacial lake outburst floods in the Himalaya. *Nature Climate Change* **9**(5), 379–383. doi:10.1038/s41558-019-0437-5

Wang X and 6 others (2012) An approach for estimating the breach probabilities of moraine-dammed lakes in the Chinese Himalayas using remote-sensing data. *Natural Hazards and Earth System Science* **12**(10), 3109–3122. doi:10.5194/nhess-12-3109-2012

Watson CS, Kargel JS, Shugar DH, Haritashya UK, Schiassi E and Furfaro R (2020) Mass Loss from Calving in Himalayan Proglacial Lakes. *Frontiers in Earth Science* **7**(January), 1–19. doi:10.3389/feart.2019.00342

Watson CS, Quincey DJ, Carrivick JL, Smith MW, Rowan AV and Richardson R (2018) Heterogeneous water storage and thermal regime of supraglacial ponds on debris-covered glaciers. *Earth Surface Processes and Landforms* **43**(1), 229–241. doi:10.1002/esp.4236

Westoby MJ, Glasser NF, Brasington J, Hambrey MJ, Quincey DJ and Reynolds JM (2014) Modelling outburst floods from moraine-dammed glacial lakes. *Earth-Science Reviews* **134**, 137–159. doi:10.1016/j.earscirev.2014.03.009

Wood JL and 20 others (2021) Contemporary glacial lakes in the Peruvian Andes. *Global and Planetary Change* **204**(November 2020), 103574. doi:10.1016/j.gloplacha.2021.103574

Yamada T and 13 others (2004) Outline of 2002: Research activities on glaciers and glacier lakes in Lunana Region, Bhutan Himalayas. *Bulletin of Glaciological Research* **21**, 79–90.

Yao X, Liu S, Sun M, Wei J and Guo W (2012) Volume calculation and analysis of the changes in moraine-dammed lakes in the north Himalaya: A case study of Longbasaba lake. *Journal of Glaciology* **58**(210), 753–760. doi:10.3189/2012JoG11J048

Zhang G and 9 others (2023c) Underestimated mass loss from lake-terminating glaciers in the greater Himalaya. *Nature Geoscience* **16**(4), 333–338. doi:10.1038/s41561-023-01150-1

Zhang G, Yao T, Xie H, Wang W and Yang W (2015) An inventory of glacial lakes in the Third Pole region and their changes in response to global warming. *Global and Planetary Change* **131**, 148–157. doi:10.1016/j.gloplacha.2015.05.013

Zhang T, Wang W and An B (2023b) A conceptual model for glacial lake bathymetric distribution. *Cryosphere* **17**(12), 5137–5154. doi:10.5194/tc-17-5137-2023

Zhang T, Wang W, An B and Wei L (2023a) Enhanced glacial lake activity threatens numerous communities and infrastructure in the Third Pole. *Nature Communications* **14**(1), 8250. doi:10.1038/s41467-023-44123-z

Zheng G and 12 others (2021) Increasing risk of glacial lake outburst floods from future Third Pole deglaciation. *Nature Climate Change* **11**(5), 411–417. doi:10.1038/s41558-021-01028-3